Photodissociation of the Phosphine-Substituted Transition Metal Carbonyl Complexes Cr(CO)$_5$L and Fe(CO)$_4$L: A Theoretical Study

T. P. M. Goumans,[†] Andreas W. Ehlers,[†] Marc C. van Hemert,[‡] Angela Rosa,[§] Evert-Jan Baerends,[||] and Koop Lammertsma*,[†]

Contribution from the Department of Chemistry, Faculty of Sciences, Vrije Universiteit, De Boelelaan 1083, NL-1081 HV, Amsterdam, The Netherlands, Leiden Institute of Chemistry, Gorlaeus Laboratoria, University of Leiden, P.O. Box 9502, NL-2300 RA, Leiden, The Netherlands, and Department of Chemistry, University of Basilicata, Via N. Sauro 85, 85100 Potenza, Italy

Received October 29, 2002 ; E-mail: lammert@chem.vu.nl

Abstract: The photochemistry of the phosphine-substituted transition metal carbonyl complexes Cr(CO)$_5$PH$_3$ and *ax*-Fe(CO)$_4$PH$_3$ is studied with time-dependent DFT theory to explore the propensity of the excited molecules to expel their ligands. The influence of the PH$_3$ ligand on the properties of these complexes is compared with the photodissociation behavior of the binary carbonyl complexes Cr(CO)$_6$ and Fe(CO)$_5$. The lowest excited states of Cr(CO)$_5$PH$_3$ are metal-to-ligand charge transfer (MLCT) states, of which the first three are repulsive for PH$_3$ but modestly bonding for the axial and equatorial CO ligands. The repulsive nature is due to mixing of the initial MLCT state with a ligand field (LF) state. A barrier is encountered along the dissociation coordinate if the avoided crossing between these states occurs beyond the equilibrium distance. This is the case for expulsion of CO but not for the PH$_3$ group as the avoided state crossing occurs within the equilibrium Cr−P distance. The lowest excited state of *ax*-Fe(CO)$_4$PH$_3$ is a LF state that is repulsive for both PH$_3$ and the axial CO. Excited-state quantum dynamics calculations for this state show a branching ratio of 99 to 1 for expulsion of the axial phosphine ligand over an axial CO ligand. The nature of the phosphorus ligand in these Cr and Fe complexes is only of modest importance. Complexes containing the three-membered phosphirane or unsaturated phosphirene rings have dissociation curves for their lowest excited states that are similar to those having a PH$_3$ ligand. Analysis of their ground-state Cr−P bond properties in conjunction with frontier orbital arguments indicate these small heterocyclic groups to differ from the PH$_3$ group mainly by their enhanced σ-donating ability. All calculations indicate that the excited Cr(CO)$_5$L and Fe(CO)$_4$L molecules (L = PH$_3$, PC$_2$H$_5$, and PC$_2$H$_3$) prefer dissociation of their phosphorus substituent over that of an CO ligand. This suggests that the photochemical approach may be a viable complement to the ligand exchange and redox methods that are currently employed to demetalate transition metal complexed organophosphorus compounds.

Introduction

The excited-state behavior of substituted carbonyl transition metal complexes M(CO)$_n$L is a relatively unexplored topic. More is known about the binary carbonyl M(CO)$_n$ complexes. These undergo CO photodissociation, which is applied as a general method for the introduction of other ligands to obtain M(CO)$_n$L.[1] Although the photophysical mechanism of this process has been the topic of experimental[2] and theoretical[3] studies, photodissociation of ligands other than a carbonyl has not received much attention. Either a CO group or ligand L

may dissociate from photoexcited M(CO)$_n$L (eq 1). Multiple replacements of CO for L ligands are observed when binary carbonyl complexes are irradiated extensively in the presence of an excess of L.[1,2] However, it is more difficult to establish whether photoexcited M(CO)$_n$L also exchanges its L ligand because of the degeneracy (L for L) under most experimental setups. We became interested in this issue as a potential method

* Address correspondence to this author.
† Department of Organic and Inorganic Chemistry, Vrije Universiteit.
‡ University of Leiden.
§ University of Basilicata.
|| Department of Theoretical Chemistry, Vrije Universiteit.

(1) (a) Geoffroy, G. L.; Wrighton, M. S. *Organometallic Chemistry*; Academic Press: New York, 1979; Chapter 2. (b) Wrighton, M. S. *Chem. Rev.* **1974**, *74*, 401. (c) Nayak, S. K.; Burkey, T. J. *J. Am. Chem. Soc.* **1993**, *115*, 6391.

(2) (a) Leadbeater, N. *Coord. Chem. Rev.* **1999**, *188*, 35. (b) Trushin, S. A.; Fuss, W.; Schmid, W. E. *Chem. Phys.* **2000**, *259*, 313. (c) Trushin, S. A.; Fuss, W.; Kompa, K. L.; Schmid, W. E. *J. Phys. Chem. A* **2000**, *104*, 1997. (d) Fuss, W.; Schmid, W. E.; Trushin, S. A. *J. Phys. Chem. A* **2001**, *105*, 333. (e) Fuss, W.; Trushin, S. A.; Schmid, W. E. *Res. Chem. Int.* **2001**, *27*, 447. (f) Snee, P. T.; Payne, C. K.; Mebane, S. D.; Kotz, K. T.; Harris, C. B. *J. Am. Chem. Soc.* **2001**, *123*, 6909.

(3) (a) Pollak, C.; Rosa, A.; Baerends, E. J. *J. Am. Chem. Soc.* **1997**, *117*, 7324. (b) Baerends, E. J.; Rosa, A. *Coord. Chem. Rev.* **1998**, *177*, 97. (c) Rubner, O.; Baumert, T.; Bergt, M.; Kiefer, B.; Gerber, G.; Engel, V. *Chem. Phys. Lett.* **2000**, *316*, 585. (d) Heitz, C. H.; Guillaumont, D.; Cote-Bruand, I.; Daniel, C. *J. Organomet. Chem.* **2000**, *609*, 67. (e) Guillaumont, D.; Vl_ek, A.; Daniel, C. *J. Phys. Chem.* **2001**, *105*, 1107. (g) Bruand-Cote, I.; Daniel, C. *Chem.—Eur. J.* **2002**, *8*, 1361.

to complement the current ligand exchange and redox methods that are of limited generality in removing the $M(CO)_n$ group from organophosphorus ligands, which hampers the applicability of the low-valent reagent $RPM(CO)_5$.[4-6]

$$M(CO)_n + L \xleftarrow{h\nu} (OC)_nM{-}L \xrightarrow{h\nu} (OC)_{n-1}M{-}L + CO \quad (1)$$
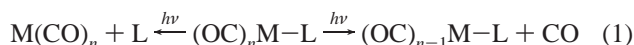
In this study we examine, by theoretical means, the photochemical dissociation channels for two phosphine-substituted transition metal carbonyl complexes, $Cr(CO)_5PH_3$ (**1**) and *ax*-$Fe(CO)_4PH_3$ (**2**). A qualitative understanding for the propensity of the photoexcited complexes to expel either PH_3 or CO is developed using time-dependent density functional theory (TDDFT). The applicability of TDDFT has been established in recent studies on the interpretation of the electronic spectra of transition metal complexes, among which $Cr(CO)_6$.[7] We further scrutinize the excited-state behavior of *ax*-$Fe(CO)_4PH_3$ with quantum dynamics. Finally, the results are generalized to other phosphorus ligands by considering the photodissociation of $Cr(CO)_5L$ and $Fe(CO)_4L$ complexes with strained phosphirane and phosphirene three-membered rings.

Computational Details

All density functional theory calculations have been performed with the parallelized ADF suite of programs, release 2000.02.[8] Geometry optimizations were carried out with the generalized gradient approximation, using nonlocal corrections to exchange by Becke[9] and to correlation by Perdew[10] (BP86). The Kohn–Sham MOs were expanded in a large, uncontracted basis set of Slater-type orbitals (STOs), of a triple-ζ + polarization functions quality (ADF basis set IV). The [He] cores of carbon and oxygen and the [Ne] core of phosphorus were treated by the frozen-core approximation. Chromium and iron were described by a frozen [Ne] core, a double-ζ 3s- shell, triple-ζ 3p-, 4s-, and 3d-shells, and a 4p-polarization function. An auxiliary set of STOs was used to fit the density for the Coulomb-type integrals.[8a] The excitation energies for each structure have been calculated with the TDDFT implementation of ADF,[11] using the asymptotically correct van Leeuwen–Baerends exchange-correlation potential (LB94)[12,13] and the adiabatic local density approximation (ALDA) for the exchange-correlation kernel. Only singlet excited states are considered. The energy of the density obtained with the LB94 potential is calculated post-SCF with the BP86 energy functional, denoted as $BP86[\rho_{(LB94)}]$. Bond

(4) (a) Lammertsma, K.; Vlaar, M. J. M. *Eur. J. Org. Chem.* **2002**, *7*, 1127. (b) Vlaar, M. J. M.; Ehlers, A. W.; de Kanter, F. J. J.; Schakel, M.; Spek, A. L.; Lammertsma, K. *Angew. Chem.* **2000**, *112*, 3071; *Angew. Chem., Int. Ed.* **2000**, *38*, 2943. (c) Wit, J. B. M.; van Eijkel, G. T.; de Kanter, F. J. J.; Schakel, M.; Ehlers, A. W.; Lutz, M.; Spek, A. L.; Lammertsma, K. *Angew. Chem.* **1999**, *111*, 2716; *Angew. Chem., Int. Ed. Engl.* **1999**, *38*, 2596.
(5) (a) Cowley, A. H. *Acc. Chem. Res.* **1997**, *30*, 445. (b) Mathey, F. *Chem. Rev.* **1990**, *90*, 997. (c) Stephan, D. W. *Angew. Chem.* **2000**, *112*, 322; *Angew. Chem., Int. Ed.* **2000**, *39*, 314.
(6) Dillon, K. D.; Mathey, F.; Nixon, J. F. *Phosphorus: The Carbon Copy*; Wiley: Chichester, U.K., 1998.
(7) Rosa, A.; Baerends, E. J.; van Gisbergen, S. J. A.; van Lenthe, E.; Groeneveld, J. A.; Snijders, J. G. *J. Am. Chem.* **1999**, *121*, 10356.
(8) (a) Baerends, E. J.; Ellis, D. E.; Ros, P. *Chem. Phys.* **1973**, *2*, 41. (b) te Velde, G.; Baerends, E. J. *J. Comput. Phys.* **1992**, *99*, 84. (c) Fonseca-Guerra, C.; Visser, O.; Snijders, J. G.; te Velde, G.; Baerends, E. J. In *METECC-95*; Clementie, E., Corongiu, C., Eds.; Cagliari, Italy, 1995; p 305.
(9) Becke, A. D. *Phys. Rev. A* **1988**, *38*, 3098.
(10) Perdew, J. P. *Phys. Rev. B* **1986**, *33*, 8822.
(11) RESPONSE, extension of the ADF program for linear and nonlinear response calculations, by S. J. A. Gisbergen, J. G. Snijders, and E. J. Baerends, with contributions by J. A. Groeneveld, F. Kootstra, and V. P. Osinga.
(12) van Leeuwen, R.; Baerends, E. J. *Phys. Rev. A* **1994**, *49*, 2421.
(13) For a comparison of TDDFT calculations with the LB94, SVWN, BLYP, and B3LYP xc-potentials, see: Hirata, S.; Head-Gordon, M. *Chem. Phys. Lett.* **1999**, *314*, 291.

Chart 1. Investigated Dissociation Modes (Dashed Lines) of **1** and **2** for Their Imposed Symmetries with All Displayed with the Same *yz*-Mirror Plane
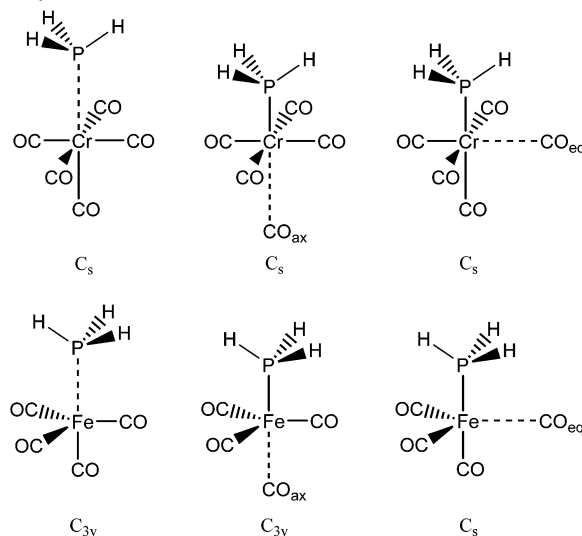
dissociation energies (BDE) are defined as the energy difference between the optimized *singlet* fragments, with imposed symmetry constraints (vide infra), and the equilibrium geometry of the complex. Singlet–triplet intersystem crossing is a forbidden and presumably slow process for these light-atom complexes.

The ground-state curves along the dissociation coordinates were determined by optimizing the structures for which the distance between the metal and its ligand were enlarged systematically while enforcing the symmetry constraints as depicted in Chart 1. The excited-state curves were obtained by calculating the vertical TDDFT-excitation energies with respect to that of the ground state. The ground-state reference is the $BP86[\rho_{(LB94)}]$ energy of the BP86-optimized geometries.

For the excited-state quantum dynamics of *ax*-$Fe(CO)_4PH_3$, a 20×20 2-dimensional grid was generated by fixing the distance of both axial ligands to the metal while maintaining $C_{3\nu}$ symmetry. Equidistant 40×40 and 384×384 grids for the ground and excited states, respectively, were created by 2D cubic spline interpolation of these data points. The grids ranged from 2.1 to 10.1 a_0 (1.1–5.3 Å) along the carbonyl dissociation coordinates and from 2.9 to 10.9 a_0 (1.5–5.8 Å) for dissociation of the phosphine. The calculations were performed with the approximated light-heavy-light (LHL) Hamiltonian[14] even though concerns arise (a) for linear alignments of constituting fragments and (b) for systems that do not have large heavy to light mass ratios.[14b] To check the introduced error, we also performed calculations in 2D Jacobi coordinates. Because the two Hamiltonians gave no significantly different results, we present those obtained for the LHL approximation for reasons of transparency. The ground-state vibrational wave function was calculated variationally from a 2×7 Morse oscillator basis using a 14×14 quadrature. The oscillator strength, as determined from TDDFT, showed little variation around the Franck–Condon region, especially along the asymmetric displacement modes. Therefore, we used a constant transition dipole moment of 0.0497 atomic units, which is the value at the equilibrium geometry.

The wave packet was propagated using the short iterative Lanczos (SIL) integrator[15] of order 8, taking 2048 time steps of 10 atomic units ($\approx$0.242 fs). The kinetic energy part of the Hamiltonian was evaluated with the fast Fourier transform algorithm.[16] To prevent reflection of the wave packet at the boundaries, an optical potential of 0.076 hartree

(14) (a) Clary, D. C.; Henshaw, J. P. In *The Theory of Chemical Reaction Dynamics*; Clary D. D., Ed.; Reidel: Dordrecht, The Netherlands, 1986; pp 331–358. (b) Kroes, G.-J. *J. Chem. Phys.* **1994**, *101*, 5792.
(15) Park. T. J.; Light, J. C. *J. Chem. Phys.* **1986**, *85*, 5870.
(16) Kosloff, D.; Kosloff, R. *J. Comput. Phys.* **1983**, *52*, 35.

Table 1. BP86 Calculated and Experimental Bond Lengths (in Å) in Chromium and Iron Complexes

bond	$Cr(CO)_6{}^a$	$Cr(CO)_5PH_3$	$Cr(CO)_5$	ax-$Cr(CO)_4PH_3$	eq-$Cr(CO)_4PH_3$
$M-PH_3$		2.358 (2.348)^b		2.272	2.364
$M-C_{ax}$	1.908 (1.918)	1.871	1.828		1.820
$C-O_{ax}$	1.156 (1.141)	1.161	1.165		1.170
$M-C_{eq}$	1.908 (1.918)	1.899^c	1.907	1.895^c	1.863, 1.892^d
$C-O_{eq}$	1.156 (1.141)	1.160^c	1.158	1.163^c	1.165, 1.162^d

bond	$Fe(CO)_5{}^e$	$Fe(CO)_4PH_3$	$Fe(CO)_4$	ax-$Fe(CO)_3PH_3$	eq-$Fe(CO)_3PH_3$
$M-PH_3$		2.234		2.142	2.255
$M-C_{ax}$	1.811 (1.811, 1.807)	1.783	1.729		1.774
$C-O_{ax}$	1.154 (1.117, 1.152)	1.159	1.162		1.163
$M-C_{eq}$	1.809 (1.803, 1.827)	1.800	1.821	1.805	1.767
$C-O_{eq}$	1.157 (1.133, 1.152)	1.163	1.159	1.167	1.169

^{a} Experimental values in parentheses.[19a] ^{b} Average bond length in the disordered crystal.[19b] ^{c} Averaged bond length. ^{d} The first value is for the CO trans to PH$_3$, and the second, for the cis CO. ^{e} The first values in parentheses refer to crystal structure data,[19c] and the second ones, to gas-phase data.[19d]

was employed at an onset of 2.0 atomic units before the actual boundaries of both coordinates. Partial cross sections, i.e. the extent of dissociation of a particular ligand, are determined from analysis of the wave packet at an asymptotic analysis line and subsequent projection on the vibrational eigenstates of the remaining fragment.[17]

Bonding analysis of the metal−ligand interactions is accomplished with the extended transition-state method (ETS).[18] According to the ETS scheme, the bond energy between the two fragments is decomposed in the following interaction terms:

$$\text{bond energy} = \Delta E_{tot} = \Delta E_{prep} + \Delta E_{Pauli} + \Delta E_{elstat} + \Delta E_{oi}$$

The total interaction energy equals the bond energy and is decomposed into several terms. The first term ΔE_{prep} is the energy required to deform the fragments to the geometries they have in the total molecule. ΔE_{Pauli} quantifies the Pauli repulsion between the electrons on the two fragments. The electrostatic attraction between the two fragments is ΔE_{elstat}. ΔE_{oi} represents the orbital interaction term, which quantifies the energy gain upon mixing of the orbitals of the two fragments. This term can be further dissected into the different symmetry classes, which are A′ and A″ in the cases we consider here.

Results and Discussion

In the first section, we evaluate the ground-state properties of Cr(CO)$_5$PH$_3$ (**1**) in relation to Cr(CO)$_6$ and examine the excited-state surfaces along the PH$_3$ and CO dissociation coordinates. In the second section, we compare the ground-state properties and photoreactivity of ax-Fe(CO)$_4$PH$_3$ (**2**) with those of Fe(CO)$_5$. The PH$_3$ vs CO dissociation from excited **2** is further evaluated with quantum dynamics calculations. In the final section, the excited-state behavior of the corresponding phosphirane and phosphirene complexes is compared to that of **1** and **2**.

A. Cr(CO)$_5$PH$_3$ (1). Geometries and Bond Dissociation Energies. The bond lengths of the ground-state geometries of **1**, Cr(CO)$_6$, and the fragment molecules Cr(CO)$_5$ and Cr(CO)$_4$PH$_3$ are listed in Table 1, together with available experimental values.[19] The geometries obtained with the BP86 functional are in reasonable agreement with those reported experimentally.[20,21]

(17) Balint-Kurti, G. G.; Dixon, R. N.; Marston, C. C. *Int. Rev. Phys. Chem.* **1992**, *11*, 317.
(18) (a) Ziegler, T.; Rauk, A. *Inorg. Chem.* **1979**, *18*, 1755. (b) Ziegler, T.; Rauk, A. *Theor. Chim. Acta* **1977**, *46*, 1.
(19) (a) Jost, A.; Reest, B.; Yelon, W. *Acta Chrystallogr.* **1975**, *B31*, 2649. (b) Huttner, G.; Schelle, S. *J. Organomet. Chem.* **1973**, *47*, 383. (c) Braga, D.; Grepioni, F.; Orpen, A. G. *Organometallics* **1993**, *12*, 1481. (d) Beagly, B.; Schmidling, D. G. *J. Mol. Struct.* **1974**, *22*, 466.
(20) Frenking, G.; Wichmann, K.; Fröhlich, N.; Grobe, J.; Golla, W.; Le Van, D.; Krebs, B.; Läge, M. *Organometallics* **2002**, *21*, 2921.

Scheme 1. Frontier Orbital Diagram for (a) Cr(CO)$_6$ and (b) **1** with PH$_3$ Depicted along the z-Axis
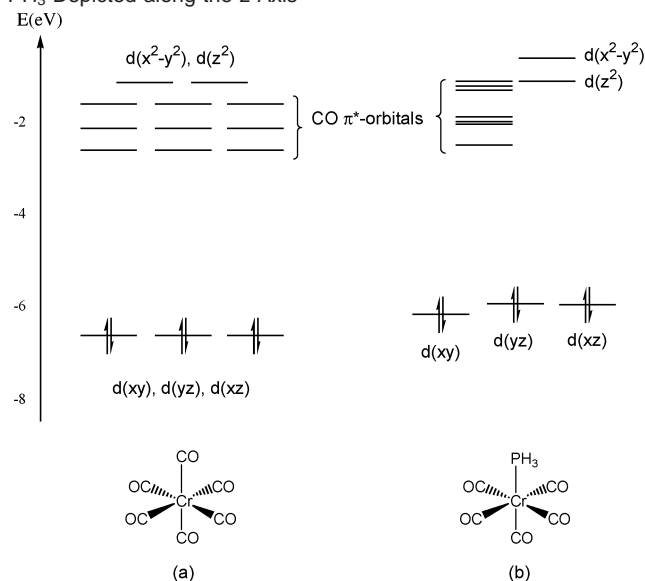
Frenking et al.[20] noted that the axial M−CO bond in M(CO)$_n$PR$_3$ is always shorter than the equatorial M−CO$_{eq}$ bonds. This is a manifestation of the competition for M → L back-bonding of ligands with a trans configuration in the transition metal complex. Because the phosphine group is a weak π-acceptor, the axial carbonyl ligand benefits from increased back-bonding to give a shorter and stronger M−CO bond. The PH$_3$ ligand also enhances M → L back-bonding to the equatorial CO ligands by destabilizing the π-orbitals attributable to the transition metal (see Scheme 1). This results in equatorial Cr−CO$_{eq}$ bond lengths that are slightly shorter in Cr(CO)$_5$PH$_3$ (1.899 Å) than in Cr(CO)$_6$ and Cr(CO)$_5$. Likewise, the Cr−PH$_3$ bond in the ax-Cr(CO)$_4$PH$_3$ fragment is shorter than in **1** (2.358 Å), as it has no trans CO group to compete for π-back-bonding.

Fragment molecule eq-Cr(CO)$_4$PH$_3$ has three types of carbonyl ligands: one axial; one equatorial trans to PH$_3$; two identical equatorial ones cis to PH$_3$. The Cr−CO$_{ax}$ bond in eq-Cr(CO)$_4$PH$_3$ is shorter than in **1** because it is trans to the unoccupied coordination site. Likewise, the trans Cr−CO$_{eq}$ bond

(21) (a) Rosa, A.; Ehlers, A. W.; Baerends, E. J.; Snijders, J. G.; Velde, G. T. *J. Chem. Phys.* **1996**, *100*, 5690. (b) Jonas, V.; Thiel, W. *J. Chem. Phys.* **1995**, *102*, 8474. (c) Wüllen, C. v. *J. Chem. Phys.* **1996**, *105*, 5485. (d) Li, J.; Schreckenbach, G.; Ziegler, T. *J. Am. Chem. Soc.* **1995**, *117*, 486.

Table 2. BP86 and BP86[$\rho_{(LB94)}$] Bond Dissociation Energies (BDEs in kcal/mol) for Chromium and Iron Complexes

theory level	ligand	$Cr(CO)_6$	$Cr(CO)_5PH_3$	$Fe(CO)_5$	$Fe(CO)_4PH_3$
BP86	PH_3		31.5		42.0
	CO_{ax}	41.7[a]	48.6	50.8	55.4
	CO_{eq}	41.7	42.2	44.9[b]	46.3
BP86[$\rho_{(LB94)}$]	PH_3		27.0		37.8
	CO_{ax}	39.4[a]	46.9	48.9	53.9
	CO_{eq}	39.4	39.7	41.3[b]	42.6

[a] The experimental CO dissociation energy for $Cr(CO)_6$ is 36.8 ± 2 kcal/mol; see ref 22. [b] The experimental CO dissociation energy for $Fe(CO)_5$ is 41.5 ± 2 kcal/mol; see ref 22.

(1.863 Å) is shorter than those that are cis to PH_3 (1.892 Å), again due to the trans phosphine effect.

The BP86 bond dissociation energies for removal of the ligands from **1** and $Cr(CO)_6$ are listed in Table 2. The BDE of 41.7 kcal/mol for $Cr(CO)_6$ is larger than the experimentally determined value of 36.8 ± 2 kcal/mol[22] but in accord with earlier theoretical estimates.[21] The BP86[$\rho_{(LB94)}$] energies follow the same trend as the BP86 energies, but they are consistently smaller by about 2−4 kcal/mol. Because the LB94 density features the correct asymptotic decay of $-1/r$ at infinity, electrons are more strongly bound to the nuclei than they are using LDA or GGA potentials,[12] which results in reduced bonding energies. Despite this better agreement (BDE = 39.4 kcal/mol) with the experimental $Cr(CO)_6$ value, BP86[$\rho_{(LB94)}$] energies should be used with caution.[23]

Because of the weak π-acceptor ability of the phosphine group, the axial carbonyl of **1** is about 6.9 kcal/mol tighter bound to the metal (BDE = 48.6 kcal/mol) than in $Cr(CO)_6$, whereas the effect on the equatorial carbonyls is only very small. The weakest bound ligand of **1** is the phosphine group with a BDE of 31.5 kcal/mol. Frenking et al., who used a slightly different basis set and included relativistic effects, reported recently a nearly identical value of 32.4.[20,24]

Excitation Energies. We compare the excitation energies of **1** with those of $Cr(CO)_6$, the excited states of which have been investigated previously by TDDFT[7] and CASPT2[25] theoretical approaches. Table 3 lists the energies of the calculated ligand field (LF) excitation and the lowest symmetry-allowed metal-to-ligand charge transfer (MLCT) excitation, which is associated with the experimentally observed low-energy absorption (vide infra).[26]

Two recent theoretical studies showed that the low-energy absorption of $Cr(CO)_6$ at 3.60 eV results from a MLCT and not a LF transition.[7,25] The initial LF assignment[26a] was based on classic ligand field theory, which assumes that the frontier orbitals of $Cr(CO)_6$ are the chromium d-orbitals, split in a t_{2g} and an e_g set. The six chromium electrons occupy the t_{2g} set with the e_g set remaining unoccupied. The lowest electronic

(22) Lewis, K. E.; Golden, D. M.; Smith, G. P. *J. Am. Chem. Soc.* **1984**, *106*, 3905.
(23) For a discussion on the limitations of this theoretical model, see: http://www.scm.com/Doc/Doc2002/ADFUsersGuide.pdf.
(24) Frenking et al.[20] also considered the staggered form of $Cr(CO)_5PH_3$, which is more stable than the eclipsed form albeit with only 0.1 kcal/mol. In this study we use the eclipsed form to conserve symmetry along the equatorial dissociation mode.
(25) Pierloot, K.; Tsokos, E.; Vanquickenborne, L. G. *J. Phys. Chem.* **1996**, *100*, 16545.
(26) (a) Beach, N. A.; Gray, H. B. *J. Am. Chem. Soc.* **1968**, *90*, 5731. (b) Braterman, P. S.; Walker, A. P. *Discuss. Faraday Soc.* **1969**, *47*, 121. (c) Dartiguenave, Y.; Dartiguenave, M.; Gray, H. B. *Bull. Soc. Chim. Fr.* **1969**, *12*, 4223.

Table 3. Selected LB94/ALDA and Experimental Singlet Excitation Energies (in eV) for $Cr(CO)_6$, $Cr(CO)_5PH_3$, $Fe(CO)_5$, and $Fe(CO)_4PH_3$

molecule	excitation energy (eV)		excited state	classification
	calc	exptl		
$Cr(CO)_6$	3.78[a]	3.60[b]	$1E_{1u}$	MLCT
	5.20[a]		$3T_{1g}$	LF
$Cr(CO)_5PH_3$	3.35	~3.45[c]	$1A'$	MLCT
	4.61		$12A'$	LF^d
$Fe(CO)_5$	3.76		$1E'$	MLCT
	3.77		$1A_2''$	MLCT
	3.93		$2E'$	LF
	4.21	4.40[e]	$3E'$	MLCT
	4.84	5.15[e]	$2A_2''$	MLCT
$Fe(CO)_4PH_3$	3.11		$1E$	LF
	3.67		$1A_1$	MLCT
	3.69		$2E$	MLCT

[a] From ref 7. The CASPT2 values are 3.41−3.59 and 4.85 eV for the first MLCT and the LF state.[25] [b] From ref 26a; vapor at 300 K. [c] From ref 26b; with PPh_3 instead of PH_3. [d] About 50% LF; also contains MLCT contributions. [e] From ref 26c; apolar solvent at 300 K.

transition then corresponds to a $t_{2g} \rightarrow e_g$ (LF) excitation. However, DFT and CASPT2 calculations showed that several CO π^*-orbitals are lower in energy than the virtual chromium orbitals. Consequently, the low-energy absorption corresponds to $t_{2g} \rightarrow \pi^*$ (MLCT) transitions, and the actual LF transition lies at much higher excitation energies.

$Cr(CO)_5PH_3$ has C_s symmetry, instead of O_h for $Cr(CO)_6$, although the metal coordination approximates C_{4v} symmetry. Consequently, all degeneracies are lifted but with some orbitals remaining close in energy (Scheme 1). The PH_3 ligand shifts all chromium d-orbitals up except the $d(z^2)$ orbital. The reduced back-donation upon CO for PH_3 substitution increases the electron density on the metal and thereby destabilizes all chromium orbitals slightly, which is most pertinent for the $d(yz)$ and $d(zx)$ orbitals. The $d(z^2)$ orbital energy remains unaffected since the electrostatic destabilization is countered by the reduction of the axial repulsive interactions upon substituting CO for PH_3.

Since the highest occupied orbitals are destabilized, the first MLCT and LF absorptions of **1** are lower in energy than those of $Cr(CO)_6$. As was the case for $Cr(CO)_6$, CO π^*-orbitals have lower energies than the virtual chromium orbitals (Scheme 1b) and therefore the lowest excited states for **1** are also MLCT states. Vertical excitation energies of 3.35−3.36 eV are calculated for the $1A'$ or $1A''$ states and 3.61 and 3.54 eV, respectively, for the $2A'$ and $2A''$ states (Table 4). The calculated lowest excitation energy for **1** (3.35 eV) is in good agreement with the observed low-energy transition of 3.45 eV for $Cr(CO)_5PPh_3$.[26b]

Photodissociation. The potential energy curves along the PH_3 and two CO dissociation modes of **1** are depicted in Figures 1−3. The $1A'$ and $1A''$ excited states are nearly degenerate along the axial displacement modes because of the approximate C_{4v} symmetry. The $2A'$ and all other (not discussed) higher lying singlet excited states are strongly bound for all ligands. The potential energy curves give insight into the tendency of the photoexcited molecule to expel one of its ligands. Besides purely repulsive excited states, photodissociation may also occur for weakly bound excited states if the barrier for this process is only modest.

The first three excited states ($1A'$, $1A''$, and $2A'$) of **1** are purely dissociative for PH_3 (Figure 1) with exothermicities of

Table 4. Excitation Energies, Barriers, and Energies of Dissociation (all in eV) for Symmetry-Allowed Excited States of Cr(CO)$_5$PH$_3$, Fe(CO)$_5$, and *ax*-Fe(CO)$_4$PH$_3$

molecule	dissoc ligand	excited state	excitation energy	barrier	dissoc energy
Cr(CO)$_5$PH$_3$	PH$_3$	1A′	3.36		−0.32
		1A″	3.35		−0.31
		2A′	3.61	1.28	1.28
		2A″	3.54		−0.29
	CO$_{ax}$	1A′	3.36	0.34	0.19
		1A″	3.35	0.33	0.18
		2A′	3.61	1.75	1.75
		2A″	3.54	0.55	0.42
	CO$_{eq}$	1A′	3.36	0.18	0.07
		1A″	3.35	0.35	0.21
		2A′	3.61	1.30	1.30
		2A″	3.54	0.33	0.25
Fe(CO)$_5$[a]	CO$_{ax}$	1E	3.76		−0.91
		1A$_1$	3.77	2.07	2.04
	CO$_{eq}$	1A$_1$	3.76	0.18	−0.12
		1B$_1$	3.76	0.08	−0.36
		1B$_2$	3.77	0.94	0.80
ax-Fe(CO)$_4$PH$_3$[a]	PH$_3$	1E	3.11		−0.74
		1A$_1$	3.67	1.66	1.66
		2E	3.69	0.21	0.21
	CO$_{ax}$	1E	3.11		−0.26
		1A$_1$	3.67	2.23	2.23
		2E	3.69	0.40	0.40
	CO$_{eq}$	1A′	3.11	0.78	0.78
		1A″	3.11	0.54	0.54
		2A′	3.67	0.78	0.78

[a] For the symmetry relationships on dissociation of the ligands, see note 29.
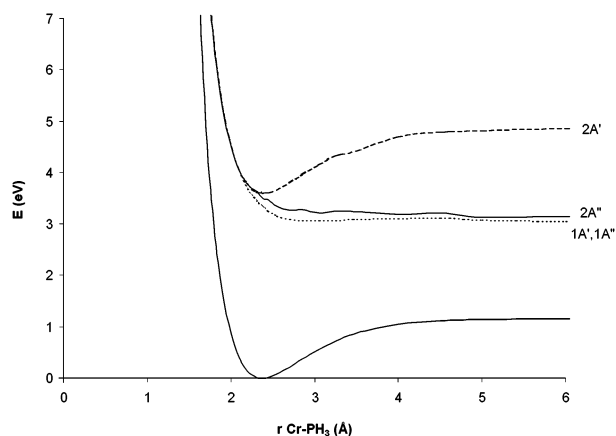
Figure 1. Ground and first excited states of Cr(CO)$_5$PH$_3$ (**1**) along the phosphine dissociation coordinate.

about 0.3 eV. In contrast, dissociating either an axial or equatorial CO ligand is slightly endothermic (0.1−0.2 eV) but also requires a small activation of up to 0.35 eV (Figures 2 and 3). The energetic data, summarized in Table 4, indicate that photoexcited **1** will expel PH$_3$ but that expulsion of CO may also be an energetically accessible process.

The dissociative character of the MLCT states of **1** seems counterintuitive, because depletion of charge from the transition metal should result in Coulombic attraction of the ligands. However, it was shown in a recent DFT-ΔSCF study that the CO dissociative nature of the lowest MLCT excited states of Cr(CO)$_6$ results from an avoided crossing of the MLCT state with the repulsive, high-energy LF state early on the Cr−CO coordinate.[3a,b]

Similar mixing of the MLCT and LF states causes the first excited state of **1** to be repulsive for PH$_3$. At shorter than the
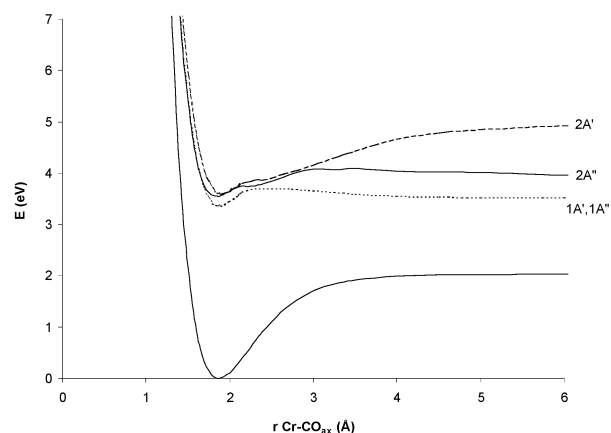
Figure 2. Ground and first excited states of Cr(CO)$_5$PH$_3$ (**1**) along the axial carbonyl dissociation coordinate.
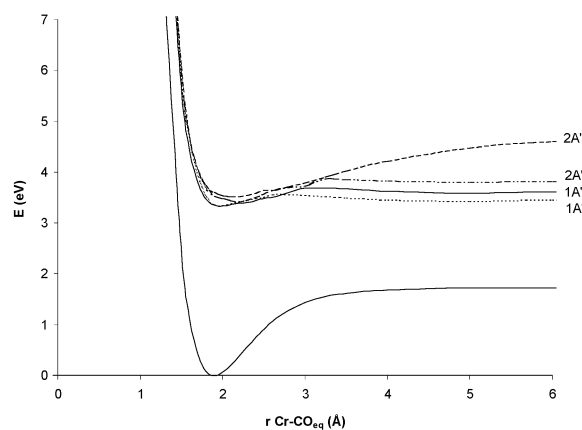
Figure 3. Ground and first excited states of Cr(CO)$_5$PH$_3$ (**1**) along an equatorial carbonyl dissociation coordinate.

equilibrium Cr−P distance, the LUMO consists mainly of CO π*-orbitals (to be associated with an MLCT state) with a higher lying virtual MO possessing Cr d(z^2) character (to be associated with an LF state), but the nature of these two orbitals fully reverses on elongating the Cr−P distance. The avoided crossing of the two states occurs farther along the CO dissociation modes than is the case for the Cr−PH$_3$ dissociation, resulting in small barriers for loss of CO. The avoided crossing of the LF and MLCT states, which is evident from the energy profiles of the unoccupied molecular orbitals of the ground state of **1** (Figure 4), occurs *within* the Cr−PH$_3$ and *beyond* the Cr−CO equilibrium distances. Apparently, PH$_3$ substitution shifts the avoided crossing to longer Cr−CO distances, presumably due to an energy lowering of the MLCT state (Table 2).

B. *ax-Fe(CO)$_4$PH$_3$ (2). Geometries and Bond Dissociation Energies.* The bond lengths of the singlet ground-state geometries of **2**, Fe(CO)$_5$, and the Fe(CO)$_4$ and Fe(CO)$_3$PH$_3$ fragment molecules are listed in Table 1 together with available experimental data.[19] The effects of CO for PH$_3$ substitution on the iron−carbonyl bond lengths parallel those of the chromium complexes; i.e., the Fe−CO$_{ax}$ bond shortens significantly (by 0.03 Å) with the Fe−CO$_{eq}$ bonds shortening only slightly. On dissociation of an equatorial CO, the remaining two Fe−CO$_{eq}$ bonds of *eq*-Fe(CO)$_3$PH$_3$ shorten by 0.03 Å because of decreased competition for π-back-bonding, which illustrates that the "trans-effect" also occurs in the equatorial plane.
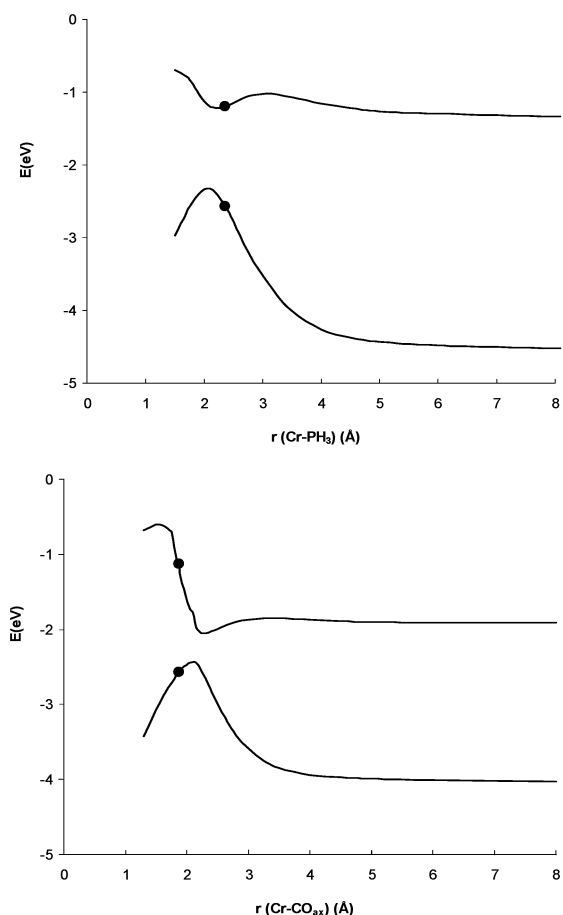
Figure 4. Energy profiles of the σ*-MO, originating from the Cr $d(z^2)$ MO and the π*-LUMO along the PH₃ (top) and CO (bottom) dissociation coordinates of Cr(CO)₅PH₃ (**1**). The solid dots indicate the equilibrium distances.

The BDEs of **2** and Fe(CO)₅ are referenced against the *singlet* fragments within their symmetry constraints (Chart 1) and are listed in Table 2.[27] As was the case for the chromium complexes, the BP86-calculated BDE for removal of an equatorial CO from Fe(CO)₅ (44.9 kcal/mol) is larger than the experimentally determined value of 41.5 ± 2 kcal/mol.[22] Although the BDE value obtained with BP86[$\rho_{(LB94)}$] (41.3 kcal/mol) is in excellent agreement with the experiment value, it should nevertheless be considered with care as noted before.[23] The PH₃ ligand stabilizes the axial CO of **2** by about 5 kcal/mol with respect to the axial CO in Fe(CO)₅, while the BDEs for the equatorial carbonyls are only slightly increased. The phosphine group is the weakest bound ligand of **2** with a BDE of 37.8 kcal/mol.

Excitation Energies. The lowest symmetry-allowed excitation energies for **2** and Fe(CO)₅ are reported in Table 3. The two experimentally observed absorptions for Fe(CO)₅[26c] are at 4.40 and 5.15 eV. Our tentative assignments for these are based on calculated excitation energies and oscillator strengths.[28] As illustrated by the orbital diagrams in Scheme 2, the iron d-orbitals, except for $d(z^2)$, are destabilized on replacing a CO

Scheme 2. Frontier Orbital Diagrams for (a) Fe(CO)₅ and (b) **2** with PH₃ Depicted along the *z*-Axis
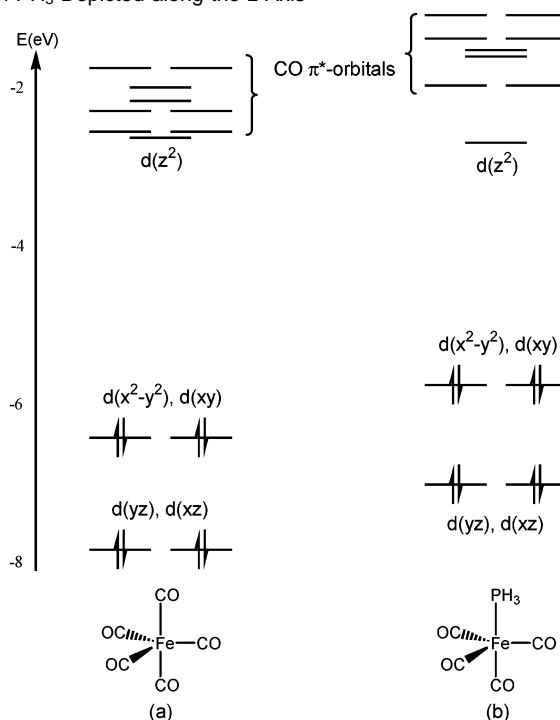
for a PH₃ ligand. Like the chromium complex, this is caused by a reduction in back-bonding, which increases the electron density at the transition metal, thereby destabilizing all frontier orbitals. The largest destabilizing effect occurs for the $d(yz)$ and $d(xz)$ orbitals ($\Delta E = 0.78$ eV) because there is one less π-acceptor along the *z*-axis. The $d(z^2)$ orbital energy is hardly affected as the PH₃ lone pair repulsive interaction, which is smaller compared to that of CO, compensates for the electrostatic effect.

The first set of CO π*-orbitals are of nearly the same energy as the virtual $d(z^2)$ orbital of Fe(CO)₅. In complex **2**, however, the CO π*-orbitals are elevated because of the increased π-back-donation to the CO ligands. The resulting relative energy difference affects the ordering of the excited states. Whereas the LF state is slightly higher in energy than two MLCT states of Fe(CO)₅ (3.93 vs 3.76–7 eV), it is by far the lowest excited state for **2** (3.11 eV). The phosphine ligand lowers the excitation energy of the LF state more than that of the MLCT states (Table 3).

Photodissociation. In discussing the expulsion of axial and equatorial carbonyls from photoexcited Fe(CO)₅, we use the symmetries for the excited states as they apply to the dissociation modes.[29] The lowest MLCT state is dissociative for all COs (1E along Fe–CO$_{ax}$ and 1E → A₁ + B₁ along Fe–CO$_{eq}$) with small energy barriers for the equatorial ones. The next higher MLCT state is bound for all COs (A₁ along Fe–CO$_{ax}$, B₂ along

(27) Singlet Fe(CO)₄ prefers a C_{2v} (seesaw) over a C_{3v} geometry by 5.9 kcal/ mol. For singlet Fe(CO)₃PH₃, the energetic preference of the C_s over C_{3v} geometry amounts to 9.1 kcal/mol. However, both fragment molecules prefer a triplet ground state, albeit with small singlet–triplet energy differences of only 0.8 and 2.1 kcal/mol for respectively Fe(CO)₄ (C_{2v}) and Fe(CO)₃PH₃ (C_s).

(28) A detailed CASSCF/MR-CCI study has reported on the excited states of Fe(CO)₅ and their importance for the dissociation processes: Rubner, O.; Engel, V.; Hachey, M. R., Daniel, C. *Chem. Phys. Lett.* **1999**, *302*, 489.

(29) The axial CO displacement in Fe(CO)₅ reduces the symmetry from D_{3h} to C_{3v}: the 1E′ excited-state correlates with 1E and the 1A₂″ state with 1A₁. The equatorial CO displacement in Fe(CO)₅ leads to C_{2v} symmetry: the E′ excited state correlates with A₁ + B₁, and the A₂″ state correlates with B₂. The equatorial CO displacement mode in **2** reduces the symmetry from C_{3v} to C_s so that the 1E state correlates with 1A′ + 1A″ and the 1A₁ state with 2A′.
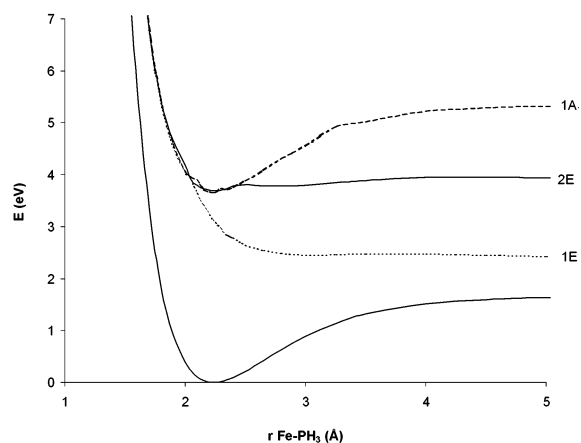
Figure 5. Ground and first excited states of *ax*-Fe(CO)$_4$PH$_3$ (**2**) along the phosphine dissociation coordinate.

Fe$-$CO$_{eq}$). The Supporting Information gives the CO$_{ax}$ and CO$_{eq}$ dissociation curves. All relevant energies for these excited-state curves of Fe(CO)$_5$ are listed in Table 4. In an earlier CI study of the excited-state curves of Fe(CO)$_5$ it was shown that the first triplet excited state $^3E'$ is dissociative for both axial and equatorial CO.[30] Our results suggest that the singlet excited state is already dissociative.

The repulsive nature of the MLCT state has different origins for the equatorial and axial COs. Upon elongation of an axial CO, the MLCT state (1E) mixes instantly with the LF state (2E), which is repulsive for the axial ligands on populating its antibonding d(z^2)-orbital. Upon elongation of an equatorial CO, MLCT$-$LF mixing also occurs, but in this case populating the d(z^2)-orbital is not repulsive. Instead, at longer Fe$-$CO distances mixing-in of the iron 4p(x/y)-orbital into the LF state underlies the repulsive nature.

The excited-state curves for Fe(CO)$_4$PH$_3$ (**2**) along the PH$_3$ dissociation mode are depicted in Figure 5, and those for removing CO$_{ax}$ and CO$_{eq}$ are given in the Supporting Material. All energetic data for the excitations and dissociations of *ax*-Fe(CO)$_5$PH$_3$ are listed in Table 4.

The first excited state for **2** is a LF state (1E: 3.11 eV) in which both axial PH$_3$ and CO ligands are unbound with exo-thermicities of 0.74 and 0.26 eV, respectively. Removal of an equatorial carbonyl from **2** is associated with an energetic barrier of 0.54 eV. This simultaneous repulsion of the axial ligands and attraction of the equatorial ligands on LF excitation, d(xy) → d(z^2) or d($x^2 - y^2$) → d(z^2), is caused by populating an orbital that is σ-antibonding with respect to the axial ligands with a concurrent depopulation of an orbital that is π-bonding and σ-antibonding with respect to the equatorial ligands. The higher excited states are MLCT states, all of which are bound for all ligands.

Excited-State Dynamics. The LF excited state of **2** is repulsive for either of its axial ligands, PH$_3$ and CO, with the higher exothermicity for expulsion of the phosphine group (Table 4). To evaluate the competitiveness of these two disso-ciation channels a quantum dynamical approach was applied by using wave packet propagation techniques. The ground- and excited-state surfaces of **2** were calculated along both axial dissociation coordinates. Their two-dimensional contour plots
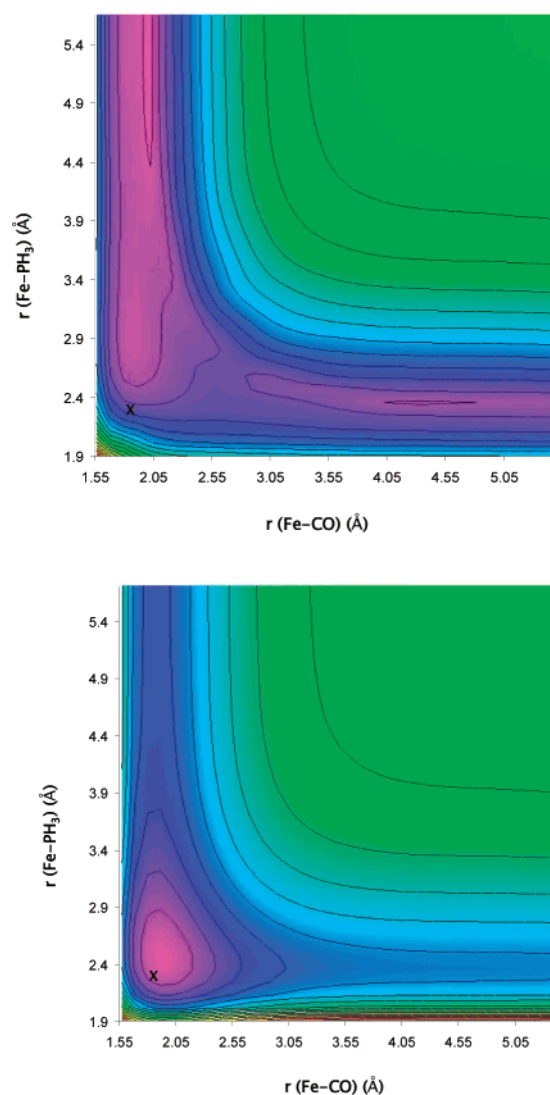

Figure 6. Contour plots of the ground- (bottom) and excited- (top) state surfaces of *ax*-Fe(CO)$_4$PH$_3$ (**2**) along the axial carbonyl and phosphine dissociation coordinates. Contour lines are separated by 0.5 eV for the ground state and by 0.17 eV for the excited state. The ground-state geometry is marked by ×.

are depicted in Figure 6. The excited-state surface demonstrates that simultaneous dissociation of both axial ligands is not possible from the LF state.

The photoabsorption cross section is determined from the ground-state vibrational wave function and the excited-state surface. The absorbance maximum is 3.08 eV, in agreement with the TDDFT value of 3.11 eV for the vertical excitation energy. The very low absorbance of 304 b ($\epsilon_0 = 0.08$ L mol^{-1} cm^{-1})[31] is compatible with the LF nature of the transition. Snapshots of the wave function amplitude visualize the evolution of the wave packet on the excited-state surfaces. In Figure 7 four snapshots are depicted for successive wave packet propaga-tion time steps of 100 atomic units ($\sim$2.4 fs). The wave packet hardly disperses on the excited state surface and almost entirely vanishes through the phosphine dissociation channel with a calculated branching ratio of $\sim$99:1.[32] These quantum dynamics

(30) Daniel, C.; Bénard, M.; Dedieu, A.; Wiest, R.; Veillard, A. *J. Phys. Chem.* **1984**, *88*, 4805.

(31) This value is derived by multiplying the absorbance with the square of the transition dipole moment that is obtained from the TDDFT calculation (0.0497 au).

(32) The calculated branching ratio of 99:1 reflects an estimate because the excited-state surface is less well defined for both ligands at larger distances.
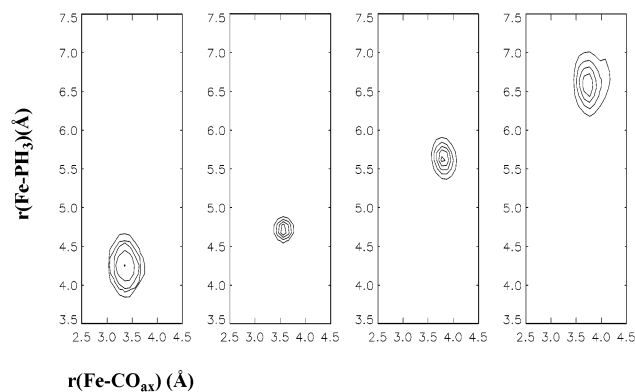
Figure 7. Motion of the wave packet on the excited-state surface of Fe-(CO)₄PH₃ (**2**) with snapshots after propagation times of 0, 100, 200, and 300 atomic time units. Contour lines give the probability $|\psi(t)|^2$ from 0.0001 to 1 in 5 steps.

Table 5. BP86 Bonding Analysis (in kcal/mol) of Cr(CO)₅−L, with L = PH₃, Phosphirane, and Phosphirene

property	PH₃	phosphirane	phosphirene
bond energy	−31.52	−31.29	−34.15
$\Delta E_{oi}(A')$	−41.74	−43.18	−44.84
$\Delta E_{oi}(A'')$	−7.47	−7.33	−8.33
ΔE_{elstat}	−64.37	−63.50	−69.69
ΔE_{Pauli}	80.77	80.76	86.66
ΔE_{prep}	1.39	1.97	2.06
$\Delta HL_\sigma{}^a$	2.00	1.61	1.01

[a] The HOMO−LUMO energy gap (in eV) for σ-interaction.

calculations indicate that PH₃ dissociation is by far the preferred pathway for LF-excited **2**. They further show that photodissociation is nearly complete within 20 fs, which is in accord with the presumption that it concerns a fast process.

C. Phosphirane and Phosphirene Complexes. The theoretical data presented so far show a preference for dissociating PH₃ from the first excited states of both **1** and **2**. It is tempting to project this behavior to any type of phosphine ligand PR₃. However, Frenking et al.[20] showed that the nature of the M−P bond is influenced appreciably by the substituent R, which may affect, of course, the photodissociation behavior. The impact of the substituent may be enhanced even further when the hybridization of the phosphorus center is altered, for example, by introducing strained ring substituents. On the other hand, the excited-state behavior of the discussed chromium and iron M(CO)ₙL complexes should be affected only modestly if the phosphorus substituent remains a strong σ-donor, weak π-acceptor ligand. To address these issues, we compare the excited-state behavior of the phosphirane- (PC₂H₅) and phosphirene-(PC₂H₃) substituted Cr and Fe complexes M(CO)ₙL with the above-discussed PH₃ ligated ones.

To establish whether the phosphorus substituents affect the ground-state properties of Cr(CO)₅L differently, we analyze their Cr−P bonding interactions (listed in Table 5) with the extended transition state method (see Computational Details), aided by an evaluation of the fragment's frontier orbital energies. Figure 8 shows the optimized geometries of CrCO₅-complexed phosphirane and phosphirene.

The frontier orbital interactions in (OC)₅Cr−PH₃, shown in Chart 2, consist of a σ-donor contribution (A′) and two metal to π-back-bonding interactions (A′ and A″). In the ETS-partitioning, the orbital interaction term ΔE_{oi} is dissected into
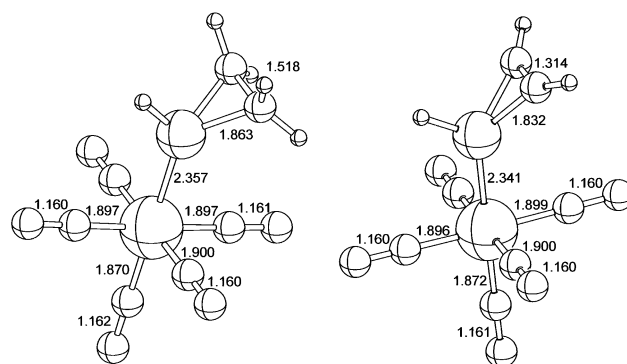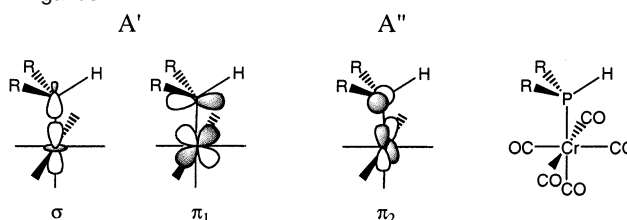

Figure 8. Bond distances (Å) in the Cr(CO)₅ complexes of phosphirane (left) and phosphirene (right).

Chart 2. Relevant Orbital Interactions between Cr(CO)₅ and P-Ligands[a]

[a] R = H (**1**), CH₂−) (phosphirane), and CH= (phosphirene). The mirror plane coincides with the surface of the paper.

two different symmetry components, i.e. A′ and A″. The $\Delta E_{oi}(A')$ term includes the σ-interaction and the π-back-bonding interaction that is symmetric with respect to the mirror plane (labeled π_1 in Chart 2), and the $\Delta E_{oi}(A'')$ consists only of the asymmetric π-back-bonding interaction (labeled π_2). For PH₃ or any C_{3v}-symmetric PR₃ ligand both π-interactions are considered equal so that the total ΔE_{oi} term can be separated into a σ-donation part and a π-back-donation part. This distinction enables a quantification of the σ,π-stabilizing properties of the PH₃ ligand (ΔE_σ and ΔE_π are 34.3 and 14.9, respectively) However, in the phosphirane and phosphirene complexes, which have C_s symmetry, the two π-interactions (π_1 and π_2) are different so that a separation of ΔE_{oi} into σ- and π-components is no longer straightforward and requires closer inspection.

The energy decomposition of the phosphirane−Cr and PH₃−Cr bonds show close resemblance (Table 5). The A′ orbital interaction energy $\Delta E_{oi}(A')$ is slightly larger for the phosphirane ligand, while the electrostatic attraction (ΔE_{elstat}) is slightly smaller. The phosphirene ligand, which has the shortest Cr−P distance (2.345 Å) of the three complexes, has both larger covalent (ΔE_{oi}) and electrostatic components than PH₃, but the ratio is the same for both. The shorter Cr−P distance of the phosphirene complex causes a higher Pauli repulsion. Both strained phosphaheterocyclic ligands have larger $\Delta E_{oi}(A')$ components for the Cr−P bond than the PH₃-ligated complex suggesting an enhancement in σ-donation.

Because the orbitals of the Cr(CO)₅ fragment of the three complexes are essentially unaffected (i.e., they have the same Cr d(z^2)-orbital energies), the enhanced $\Delta E_{oi}(A')$ likely originates from the higher lone pair orbital energies of the cyclic phosphorus fragments. The HOMO−LUMO energy gap (ΔHL_σ) is related to this difference in σ-donation. The phosphorus lone pair energy increases in the order PH₃ < phosphirane <

Table 6. Excitation Energies (eV) of Lowest Excited States in PH$_3$-, Phosphirane-, and Phosphirene-Substituted Transition Metal Carbonyls of Chromium and Iron

	Cr(CO)$_5$L			Fe(CO)$_4$L		
state	PH$_3$	PC$_2$H$_5$	PC$_2$H$_3$	PH$_3$[a]	PC$_2$H$_5$	PC$_2$H$_3$
A′	3.36	3.40	3.39	3.11	3.06	2.97
A″	3.35	3.13	3.21	3.11	3.03	3.01

[a] 1st excited state is E-symmetric, which corresponds to A′ and A″ in the substituted complexes.

phosphirene, thereby decreasing ΔHL_σ and enhancing σ-donation (Table 5).

The nature of the phosphorus ligand also affects the metal to π-back-donation but less significantly. The A′-symmetric π*-orbital (labeled π_1 in Chart 2) is almost isoenergetic for the PH$_3$ and phosphirane fragments but 0.5 eV higher in energy for the unsaturated phosphirene ligand due to mixing with the filled C=C π-orbital. The orbital energy of the A″-symmetric π*-orbital (labeled π_2 in Chart 2) decreases slightly in the order PH$_3$ < phosphirane < phosphirene, which should enhance ΔE_{oi}(A″) accordingly. Only for the phosphirene complex is this enhanced back-donation observed (Table 5).

The stronger σ-donating phosphaheterocycles increase the electron density at the metal center, which causes all orbitals to destabilize with respect to the PH$_3$ ligated complex. The Cr d(xy) orbital, which is orthogonal to the plane containing the P−H bond, is the most destabilized orbital of the phosphirane and phosphirene complexes due to the repulsive interactions with the occupied three-membered ring orbitals. As a result, the energy required for any excitation from this Cr d(xz) orbital is diminished. This is reflected in the 0.22 and 0.15 eV lower Cr d(xz) → CO π* (1A″) excitation energies for the phosphirane and phosphirene complexes, respectively, as compared to PH$_3$ complex **1**. For the corresponding iron complexes, the energies required for excitation to the first excited state (LF) are also less for the phosphaheterocyclic complexes than for PH$_3$ complex **2**. The first excitation energies for all Cr and Fe complexes are summarized in Table 6. It is noted that the $\pi \rightarrow \pi$* excitation of the phosphirene C=C double bond is not photoactive in either the LF or MLCT region of excitations, as its absorption is in the far UV, i.e. 6.34 eV for the Cr complex.

Aside from these minor differences in the excitation energies, *the axial ligands in the phosphirane and phosphirene complexes display the same photoreactivity as that of the PH$_3$-containing models*. This is illustrated by the potential energy curves along the axial Cr−P and Cr−CO$_{ax}$ dissociation coordinates for the phosphirene−Cr(CO)$_5$ complex (Figure 9). The first excited states (A′ and A″) are repulsive for the phosphirene ligand and display a small barrier for expulsion of an axial CO group. This behavior is reminiscent to that of **1**, which was discussed in section A. The potential energy curves for the lowest excitations of Fe(CO)$_4$-complexed phosphirane and phosphirene are likewise similar to those of **2** (see Supporting Information). On the basis of the bonding analysis of the ground states and the potential energy curves of the excited states, we conclude that photodissociative behavior of the phosphaheterocyclic complexes is similar to the PH$_3$-containing Cr(CO)$_5$L and Fe(CO)$_4$L complexes **1** and **2**. Thus, also on low-energy excitation of the phosphirane- and phosphirene-substituted chromium and iron carbonyl, expulsion of the phosphorus-containing ligand is favored over removal of a CO group.
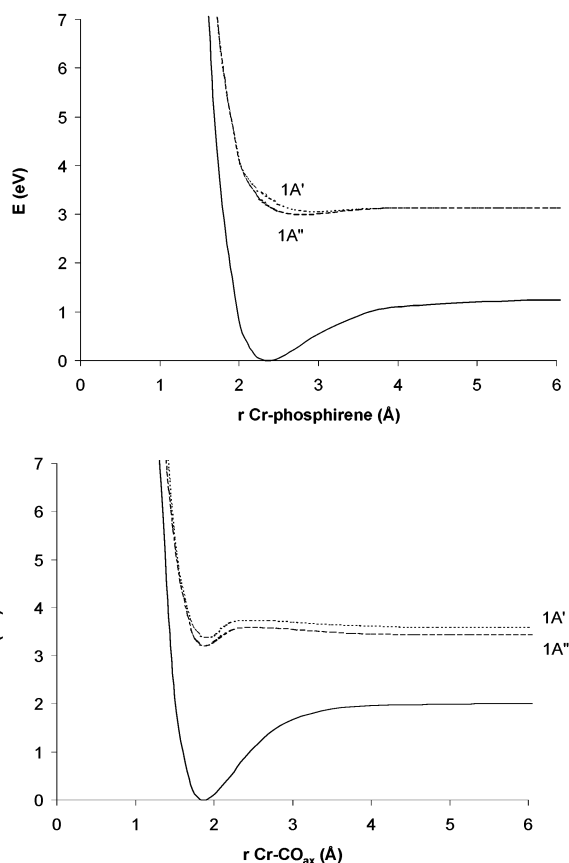
Figure 9. Ground and excited states of phosphirene−Cr(CO)$_5$ along the phosphirene (top) and axial CO (bottom) dissociation curves.

Conclusions

The photodissociation of the phosphine-substituted transition metal complexes Cr(CO)$_5$PH$_3$ and *ax*-Fe(CO)$_4$PH$_3$ was examined with TDDFT. Both have first excited states that are dissociative for the phosphine ligand, but they differ in character. The first excited states of Cr(CO)$_5$PH$_3$ are MLCT states of which the first three are dissociative for PH$_3$. Expulsion of a carbonyl ligand from these states requires only a small barrier. For *ax*-Fe(CO)$_4$PH$_3$ the first excited state is a LF state, which is dissociative for both the phosphine ligand and the axial carbonyl, while the expulsion of an equatorial carbonyl is associated with a significant barrier. Quantum dynamics calculations on the two-dimensional excited-state surface along the axial dissociation coordinates of *ax*-Fe(CO)$_4$PH$_3$ show that dissociation of the phosphine group is favored over removal of a carbonyl with a branching ratio of 99:1.

The theoretical results indicate a preference for PH$_3$ over CO dissociation from both these excited complexes. The PH$_3$ group is a weaker π-acceptor ligand than CO, which has two major consequences for the properties of M(CO)$_n$PH$_3$ as compared to the all carbonyl transition metal complexes. First, due to its superior metal to π-back-bonding, the axial CO (trans) benefits from the presence of the PH$_3$ ligand by shortening and strengthening its M−CO bond; the equatorial COs are much less affected. The phosphine group is always the weakest bound ligand. Second, the transition metal d-orbitals are destabilized by the PH$_3$ group, except for the d(z^2) orbital which is a σ-antibonding orbital along the metal phosphine axis.

The three-membered phosphirane and phosphirene ligands behave similarly to the PH_3 ligand in these transition metal complexes.

The TDDFT results for $Cr(CO)_6$, $Cr(CO)_5L$, $Fe(CO)_5$, and $Fe(CO)_4L$ (L = PH_3, PC_2H_5, and PC_2H_3) give detailed insight into the photodissociation process. Only low-energy excited states of the phosphine containing complexes are dissociative. The ligand field nature causes these excited states to be repulsive for one or more of its ligands. The LF state is directly populated *only* for the low-energy excited $Fe(CO)_4PH_3$. For all other dissociative or modestly bound excited states the initially populated MLCT state mixes with the LF state, which, depending on the position of the (avoided) crossing along the dissociation coordinate, can result in a small barrier.

Supporting Information Available: Ground- and excited-state potential energy curves for the CO_{ax} and CO_{eq} dissociation coordinates of $Fe(CO)_5$ and $Fe(CO)_4PH_3$ and for the PC_2H_5, PC_2H_3, and CO_{ax} dissociation coordinates of $Cr(CO)_5PC_2H_5$, $Fe(CO)_4PC_2H_5$, and $Fe(CO)_4PC_2H_3$ and BP86 Cartesian coordinates and BP86 and BP86[ρ_{LB94}] energies of all ground-state equilibrium geometries and fragments. This material is available free of charge via the Internet at http://pubs.acs.org.

JA029135Q